

Numerical Analysis of Short Pulse Optical Parametric Amplification Using Type I Phase Matching*

A. Dement'ev¹, O. Vrublevskaja¹, V. Girdauskas², R. Kazragytė²

¹Institute of Physics, Savanorių 231, 2028 Vilnius, Lithuania
aldement@ktl.mii.lt, oksana@ar.fi.lt

²Vytautas Magnus University, Vileikos 2, 3000 Kaunas, Lithuania
v.girdauskas@gmd.vdu.lt, r.kazragyte@gmf.vdu.lt

Received: 26.11.2003

Accepted: 23.12.2003

Abstract. The possibilities of efficient amplification and additional shortening of faster moving short fundamental harmonic pulses by the more slowly moving longer second harmonic pulses for type I phase matching are numerically analyzed for initially collimated axially symmetric beams, taking into account diffraction, group velocity mismatch and dispersion of the pulses.

Keywords: short pulses, optical parametric amplification, group velocity mismatch.

1 Introduction

The possibilities to compress the sum frequency pulses (in particular, the second harmonic pulses) during type II processes that are quadratic with respect to the field variables [1]–[3] are well known (see [4] and references therein). A concept of chirped pulse optical parametrical amplification (CPOPA) [5] attracts a great deal of attention [6]–[17]. Due to complexity of the CPOPA problem, the numerical analysis in the cited works is usually performed for type II interaction in the plane wave approximation and neglecting the group velocity mismatch of the pulses. The plane wave approximation does not

*This work has been partially supported by the Lithuanian State Science and Studies Foundation within the framework of the EUREKA project EU 2359 CHOCLAB II.

enable to analyze the beam quality changes [4] during the amplification process, and neglecting of the group velocity mismatch does not provide the possibility to correctly describe the reconversion of pulse energies during the amplification process [18]. Also note that although the theoretical analysis of amplification is usually carried out, as stated above, for type II interaction, most experiments involve type I interaction because large gain bandwidth can be realized when the OPA approaches degeneracy in type I phase matching in the case of group velocity matching between the signal and idler pulses. Therefore, type I phase matching is used to achieve the shortest pulses [12]. It should be noted that the parametric amplification is experimentally implemented in stages [7]–[12] and in each stage, the amplification saturation mode must be ensured. It increases the overall energy efficiency and, most importantly, the energy stability. Therefore, the numerical research of parametric amplification during type I interaction of very short pulses of the first harmonic and the second harmonic of even the same initial duration is an important problem. We will stress a recently demonstrated and less known possibility that, using the cascaded $\chi^{(2)} : \chi^{(2)}$ processes [19] shortening of the first harmonic pulses can also be achieved for type I interaction [20]–[26], that is unfortunately implemented with low energy efficiency. On the other hand, taking into account the group velocity mismatch, the possibility appears to efficiently amplify this short first harmonic pulse by means of a slower and longer second harmonic pulse. As it will be demonstrated below, the fundamental harmonic (FH) pulse can shorten noticeably near the beam optical axis during the optical parametric amplification in type I interaction. Therefore, analogously to the case of the stimulated Brillouin scattering [27], significantly shortened FH pulses of good spatial quality can be generated using soft Gaussian diaphragms.

2 Mathematical model and numerical method

The scheme of the FH pulse amplification using type I interaction is presented in Fig. 1.

Unlike the case of the conventional second harmonic generation [28, 29], the intense second harmonic pulse is fed to the input of the nonlinear crystal in addition to the fundamental harmonic. The electric field of the fundamen-

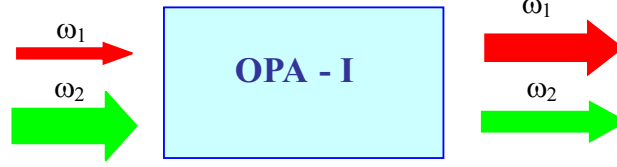


Fig. 1. The scheme of FH pulse optical parametric amplification using type I interaction.

tal and the second harmonics (SH) pulses incident upon the crystal with the mutually perpendicular polarizations vectors $\mathbf{e}_{1,2}$ can then be expressed in the following form:

$$\mathbf{E}(R, Z, T) = \text{Re} \left\{ \mathbf{e}_1 A_1(R, Z, T) e^{i(k_1 Z - \omega_1 T)} + \mathbf{e}_2 A_2(R, Z, T) e^{i(k_2 Z - \omega_2 T)} \right\}. \quad (1)$$

Here, $R = (X^2 + Y^2)^{1/2}$ and Z are the transverse and longitudinal spatial coordinates, T is the temporal coordinate, A_1 and A_2 are the slowly varying complex amplitudes of these waves, k_1 and k_2 are their wave numbers, ω_1 and $\omega_2 = 2\omega_1$ are their cyclic frequencies. Dimensional equations governing the second harmonic generation (SHG) and discussions of the expressions taking into account the contribution of the Kerr-type cubic nonlinearity are presented in our paper [29]. We shall note here that the peculiarities of the cubic phase cross-modulation of pulses in nonlinear crystals are also discussed in detail in [20, 21]. In this work, basically the same as in [29], equations were used for numerical modelling of OPA additionally taking into account the second order group-velocity dispersion (GVD). The normalized equations for the slowly varying amplitudes have the form

$$\begin{aligned} \frac{\partial a_1}{\partial z} + \frac{Z_0}{V_1 T_0} \frac{\partial a_1}{\partial t} + i \frac{\tau_{10}^2 Z_0}{4L_{DS1}} \frac{\partial^2 a_1}{\partial t^2} - i \frac{w_{10}^2 Z_0}{4L_{D1}} \frac{1}{r} \frac{\partial}{\partial r} \left(r \frac{\partial a_1}{\partial r} \right) \\ = i \frac{Z_0}{L_{NL}} a_1^* a_2 e^{-i\pi z Z_0 / L_K} + i \frac{Z_0}{2L_{PH1}} (|a_1|^2 + \beta_{12} |a_2|^2) a_1, \end{aligned} \quad (2)$$

$$\begin{aligned} \frac{\partial a_2}{\partial z} + \frac{Z_0}{V_2 T_0} \frac{\partial a_2}{\partial t} + i \frac{\tau_{20}^2 Z_0}{4L_{DS2}} \frac{\partial^2 a_2}{\partial t^2} - i \frac{w_{20}^2 Z_0}{4L_{D2}} \frac{1}{r} \frac{\partial}{\partial r} \left(r \frac{\partial a_2}{\partial r} \right) \\ = i \frac{Z_0}{L_{NL}} a_1^2 e^{i\pi z Z_0 / L_K} + i \frac{Z_0}{2L_{PH2}} (\beta_{21} |a_1|^2 + |a_2|^2) a_2, \end{aligned} \quad (3)$$

where $a_{1,2} = A_{1,2}/A_0$ are the slowly varying dimensionless complex amplitudes of the first and second harmonics normalized to the characteristic amplitude $A_0 = \sqrt{8\pi I_0/cn_1}$, I_0 is the normalization intensity, $t = T/T_0$, $z = Z/Z_0$, $r = R/R_0$ are the normalized independent coordinates, $\tau_{10,20} = T_{1,2}/T_0$ are the normalized initial pulse durations of the fundamental and second order harmonics, $L_{DS1,2} = T_{1,2}^2/2k_{1,2}''$ are the dispersion lengths, $T_{1,2}$ are the durations of the pulses ($T_2 > T_1$), $k_{1,2}'' = \partial^2 k/\partial\omega^2|_{\omega_{1,2}}$ are dispersive spreading parameters, $w_{10,20} = W_{1,2}/R_0$ are the normalized initial beam radii, $L_{D1,2} = k_{1,2}W_{1,2}^2/2$ are the diffraction lengths, $L_{NL} = 1/(\sqrt{\sigma_1\sigma_2}A_0)$ is the nonlinear length, $\sigma_{1,2} = \frac{4\pi\omega_1 d_{eff}^{(I)}}{cn_{1,2}}$ is the nonlinear coupling coefficient, $d_{eff}^{(I)}$ is the effective nonlinear susceptibility, $L_K = \pi/\Delta k$ is the coherence length, $L_{PH1,2} = 1/(k_{1,2}\bar{n}_2^{(1,2)}I_0)$ are the nonlinear phase change lengths, $\bar{n}_2^{(1,2)}$ are the nonlinear refraction indices of the medium, $\beta_{12,21}$ are the phase cross-modulation coefficients due to the Kerr effect. For the following discussion it is convenient to introduce the pulse walk-off length $L_{GVM} = T_2V_{21}$ due to group velocity mismatch (GVM) $V_{21} = \frac{1}{V_2} - \frac{1}{V_1}$, where $V_{1,2}$ are the group velocities of the fundamental and second harmonic pulses ($V_1 > V_2$).

Ranges of the normalized variables are $0 \leq t \leq t_m$, $0 \leq z \leq z_m$, $0 \leq r \leq r_m$. The boundary conditions for equations (2), (3) are as follows: $\partial a_{1,2}(r=0, z, t)/\partial r = 0$, $a_{1,2}(r=r_m, z, t) = 0$, $a_{1,2}(r, z=0, t) = a_{10,20}(r, t)$.

Let us discuss briefly the scheme of the split-step (SS) method used for solving the set of equations of the second harmonic and the first harmonic. It is convenient to apply the SS method for the set of equations (2), (3) rewritten in the following form:

$$\frac{\partial a_1}{\partial z} = \widehat{L}_{11}a_1 + \widehat{L}_{12}a_2 + \widehat{L}_{13}a_3 + \widehat{L}_{14}a_4, \quad (4)$$

$$\frac{\partial a_2}{\partial z} = \widehat{L}_{21}a_1 + \widehat{L}_{22}a_2 + \widehat{L}_{23}a_3 + \widehat{L}_{24}a_4. \quad (5)$$

Here, the operators on the right-hand side \widehat{L}_{ij} ($i = 1, 2$, $j = 1, 2, 3, 4$) describe:

$$\widehat{L}_{i1}a_i = -v_i \frac{\partial a_i}{\partial t} - ig_i \frac{\partial^2 a_i}{\partial t^2} \quad (6)$$

the group velocity mismatch and dispersion,

$$\widehat{L}_{i2}a_i = i\mu_i \frac{1}{r} \cdot \frac{\partial}{\partial r} \left(r \frac{\partial}{\partial r} \right) a_i \quad (7)$$

the beam diffraction,

$$\widehat{L}_{13}a_1 = i\gamma_1 a_1^* a_2 e^{-i\Delta z} \quad \text{and} \quad \widehat{L}_{23}a_2 = i\gamma_2 a_1^2 e^{i\Delta z} \quad (8)$$

the OPA process,

$$\begin{aligned} \widehat{L}_{14}a_1 &= i\beta_1 (|a_1|^2 + \beta_{12}|a_2|^2) a_1, \\ \widehat{L}_{24}a_2 &= i\beta_1 (\beta_{21}|a_1|^2 + |a_2|^2) a_2 \end{aligned} \quad (9)$$

the interaction of the FH and the SH due to the Kerr nonlinearity of the medium. New notations are introduced here for convenience:

$$\begin{aligned} v_i &= Z_0/V_i T_0, \quad g_i = k_i'' Z_0/2T_0^2, \quad \mu_i = Z_0/2k_i R_0^2, \\ \gamma_i &= Z_0/L_{NL}, \quad \beta_i = Z_0/2L_{PHi}, \quad \Delta = \pi Z_0/L_K. \end{aligned}$$

When numerically solving equations (4) and (5), the medium was divided into the layers of equal thickness h and the finite-difference equations were solved successively in each layer:

$$\begin{aligned} u_1 &= \Lambda_{11}a_1^n, \quad u_2 = \Lambda_{12}a_2^n, \\ v_1 &= hu_1 + \Lambda_{21}u_1, \quad v_2 = hu_2 + \Lambda_{22}u_2, \\ w_1 &= hv_1 + \Lambda_{13}v_1, \quad w_2 = hv_2 + \Lambda_{23}v_2, \\ a_1^{n+1} &= \Lambda_{14}w_1, \quad a_2^{n+1} = \Lambda_{24}w_2, \end{aligned} \quad (10)$$

Here, a_i^n , $i = 1, 2$ is the numerical approximation of the differential solution after the n -th layer of the medium $z_n = nh$, $n = 0, 1, \dots, N$, $hN = z_m$, u_i , v_i , w_i are the interim solutions.

The finite-difference approximations Λ_{ij} of the operators \widehat{L}_{ij} are as follows:

$$\Lambda_{1i}a_i^n = \text{FFT} \left[\text{FFT}[a_i^n]^{+1} \exp(-i(v_i\omega - g_i\omega^2)h) \right]^{-1}. \quad (11)$$

Here, FFT[]^{±1} are the forward and inverse discrete fast Fourier transform with respect to the temporal variable t , and ω is the frequency of the Fourier spectrum;

$$\Lambda_{2i}u_i = \frac{i2\mu_i}{\tau_+ + \tau_-} \left(\frac{\bar{u}_{i+} - \bar{u}_i}{\tau_+} - \frac{\bar{u}_i - \bar{u}_{i-}}{\tau_-} + \frac{1}{r} \frac{\bar{u}_{i+} - \bar{u}_{i-}}{2} \right), \quad (12)$$

where $\bar{u}_i = 0.5(v_i + u_i)$, $u_{\pm} = u(r \pm \tau_{\pm})$, $\tau_+ = r_{k+1} - r_k$, $\tau_- = r_k - r_{k-1}$, r_k are the coordinates of the radial grid with the density increasing towards $r = 0$: $r_k = (e^{\alpha R_k} - 1)/(e^{\alpha} - 1)$, $k = 0, 1, \dots, K$, $R_k = k\Delta R$, $\Delta RK = r_m$, $\alpha > 0$ is the grid density increase ratio;

$$\Lambda_{13}v_1 = ih\gamma_1 \bar{v}_1^* \bar{v}_2 \exp(-i\Delta\bar{z}), \quad (13)$$

$$\Lambda_{23}v_2 = ih\gamma_2 \bar{v}_1^2 \exp(i\Delta\bar{z}), \quad (14)$$

where $\bar{v}_i = 0.5(w_i + v_i)$, $\bar{z} = z + 0.5h$ and

$$\Lambda_{14}w_1 = w_1 \exp(i\beta_1(|w_1|^2 + \beta_{12}|w_2|^2)h), \quad (15)$$

$$\Lambda_{24}w_1 = w_2 \exp(i\beta_2(\beta_{21}|w_1|^2 + |w_2|^2)h). \quad (16)$$

In order to increase the accuracy of the numerical method to the second order, symmetric SS scheme (8) was applied, when finite-difference equations (10) are solved in opposite order in the adjacent layers.

3 Modeling results

When modeling the second harmonic generation and the fundamental harmonic amplification processes, the amplitude envelopes of the input FH and SH pulses possessed the Gaussian transverse distribution and the Gaussian temporal envelope and plane wavefront:

$$a_j(r, z=0, t) = a_{j0} \exp\left(-r^2/w_{j0}^2 - 2 \ln 2(t - t_{jC})^2 \tau_{j0}^2\right), \quad (j = 1, 2), \quad (17)$$

where $a_{j0} = |a_{j0}| \exp(i\varphi_{j0})$ are the normalized amplitudes of the FH and SH pulses, φ_{j0} are the input phases, w_{j0} are their normalized radii at the level of $1/e^2$ of the peak intensity, τ_{j0} are the normalized pulse durations of the

harmonics at half the peak intensities, t_{jC} are the moments of appearance of the pulse peaks.

A KDP crystal with the group velocity mismatch $V_{21} \approx 77$ fs/mm and the nonlinear refraction index $\bar{n}_2^{(1,2)} \approx 0.27 \times 10^{-19}$ m²/W for $\lambda_1 = 800$ and $\lambda_2 = 400$ nm were selected for modeling. These and other data necessary for calculations were taken from the monograph [28]. The pulse durations were selected $T_1 = 50$ fs and $T_2 = 200$ fs, so that the influence of the group velocity mismatch on the efficiency and quality of the amplified FH pulse could be investigated. The temporal normalization constant was selected to be $T_0 = 1000$ fs, due to considerations of the graphical representation of the calculation results, and the longitudinal normalization constant was $Z_0 = V_2 T_0$. The radii of Gaussian beams of the harmonics were large enough (~ 1 cm), therefore, the effect of the beam diffraction on the amplification process was insignificant. The diffraction terms with transverse Laplacians were still taken into account exactly in the equations, to be able to calculate precisely the changes of the beam propagation factors [4, 27, 29]. The calculation results presented below were obtained for the intensities of second harmonic for which the relation $Z_0/L_{NL} = 0.5$ was satisfied. The input phases of pulses were set $\varphi_{10} = 0$ and $\varphi_{20} = \pi/2$ for the effective amplification of fundamental harmonic. Note as well that, although the developed algorithm and the program, as follows from the above, provide the possibility of calculations taking into account the Kerr nonlinearity, utilization of longer and consequently less intense pulses of the second harmonic reduces this influence. Therefore, in this work, the results that have been obtained without taking into account the phase self- and cross-modulation of the pulses are presented.

By changing the pulse delay t_{jC} , the energy efficiency of the amplification process or the temporal pulse compression can be optimized. Fig. 2 presents the results of pulse propagation calculations in the absence of interaction. It is seen that the propagating SH pulse ($a_{20} = 1.0$, $t_{2C} = 0.5$) to which the coordinate system is fixed remains virtually unchanged due to diffraction and dispersive spread. At the same time, a shorter and faster FH pulse, initially delayed by $t_{1C} = 0.6$, runs practically through the entire SH pulse and spreads only slightly due to the influence of the medium dispersion, since the influence

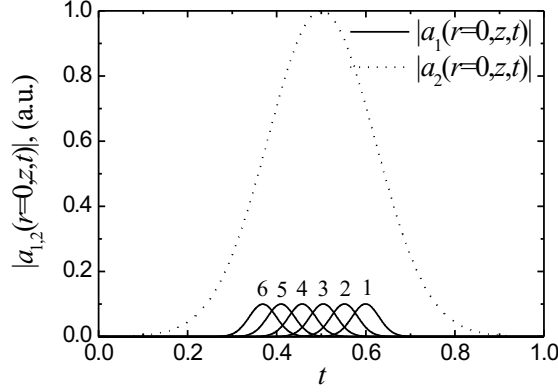


Fig. 2. The FH pulse propagation through the SH pulse due to the group velocity mismatch taking into account dispersion of the pulses at different planes along propagation: curve 1 ($z = 0$), curve 2 ($z = 3$), curve 3 ($z = 6$), curve 4 ($z = 9$), curve 5 ($z = 12$), curve 6 ($z = 15$).

of diffraction is insignificant, the same way as for the SH pulse. Note that in this figure, the modules of the complex amplitudes that usually give a picture of finer details of changes of the spatio-temporal shape are presented. However, in this case, due to smallness of both the FH amplitude itself, as well as the smallness of the dispersional spreading, its changes are difficult to make out. Only in the figure of larger scale, it can be noticed that the pulse at the exit from the medium (curve 6, $z = 15$) is slightly lower than the pulse at the entrance to the medium (curve 1, $z = 0$).

Changes of the spatio-temporal intensity distributions of the FH and SH during the amplification process in various cross-sections of the crystal are presented in Fig. 3. It is seen that the intensity of the first harmonic grows by a large factor, while significant reduction of the pulse duration on the beam axis begins as the energy reconversion from the trailing part of the pulse into the second harmonic starts. It is worth noting, however, that initially only the energy redistribution within the pulses takes place, while the integral energy of the pulse being amplified grows. As the pulses propagate further, integral energy conversion from the first harmonic to the second harmonic begins. Fig. 4 depicts the pulse structure exactly at the beginning of this stage. It is seen (Fig. 4) that the secondary peak in the second harmonic increased noticeably during reconversion, and the first harmonic pulse assumed the shape

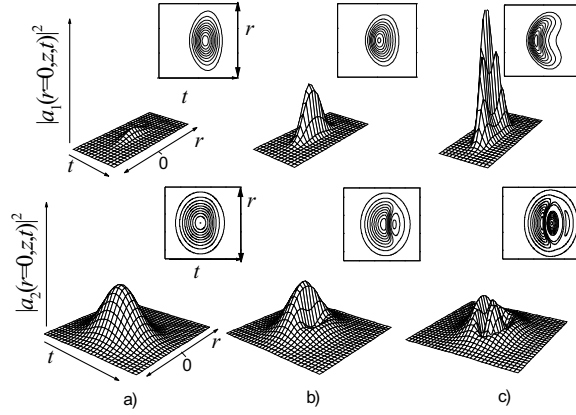


Fig. 3. Spatio-temporal structure of normalized intensity of the FH ($a_{10} = 0.1$, $t_{1C} = 0.7$) and SH ($a_{20} = 1.0$, $t_{2C} = 0.5$) pulses and their isolines at the different distances inside the crystal: a) $z = 6$, b) $z = 9$, c) $z = 12$.

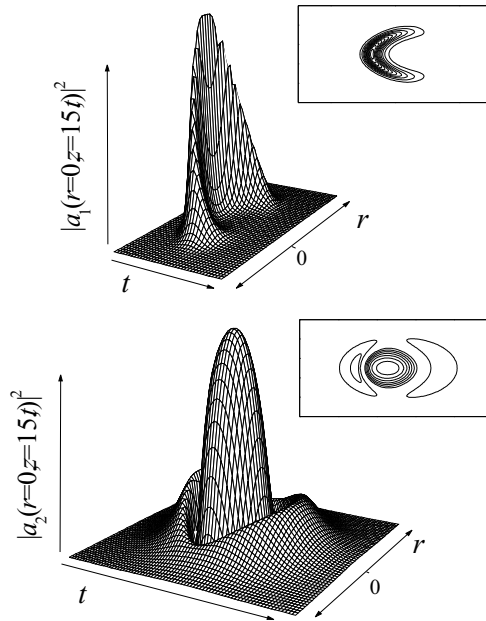


Fig. 4. Spatio-temporal structure of normalized intensity of the fundamental and second harmonic pulses and their isolines at the exit $z = 15$ from the crystal.

characteristic of the compression regime, analogous to the shape of the Stokes pulse in the compression regime [27].

Changes of the pulse shapes of instantaneous power and axial intensity in various cross-sections along the propagation direction are presented in Fig. 5. It is seen that the pulse shape of the second harmonic becomes strongly jagged,

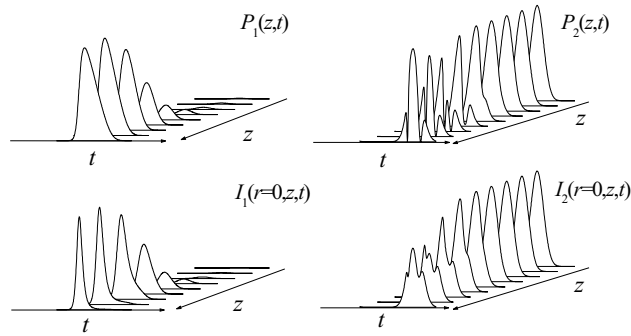


Fig. 5. The power $P_{1,2}(z, t)$ and intensity $I_{1,2}(r = 0, z, t)$ envelopes of the FH and SH pulses at the different distances inside the crystal.

and the duration of the near-axial part of the FH pulse decreases significantly during the amplification process. However, the duration of the instantaneous power pulses, or, in other words, the integral pulse duration, increases due to formation of the ring-shaped pulse structures.

The energy conversion coefficient indicating which part of energy is transferred from the second harmonic pulse to the fundamental harmonic pulse was used for the analysis of the modeling results of the fundamental harmonic amplification:

$$\eta_1(z) = \frac{\iint |a_1(r, z, t)|^2 dt dr - \iint |a_1(r, z = 0, t)|^2 dt dr}{\iint |a_2(r, z = 0, t)|^2 dt dr}. \quad (18)$$

The energy portion remaining in the second harmonic was defined by the

expression

$$\eta_2(z) = \frac{\iint |a_2(r, z, t)|^2 dt dr}{\iint |a_2(r, z = 0, t)|^2 dt dr}. \quad (19)$$

Taking into account that the initial energy of the incident pulse of the fundamental harmonic amounted to only 0.25% of the energy of the second harmonic pulse, the sum of these coefficients is equal to $\eta_1 + \eta_2 \cong 1$ in every plane. Fig. 6 presents the changes of the energy conversion coefficients along the propagation direction. It is seen that at $z \sim 15$, the integral energy

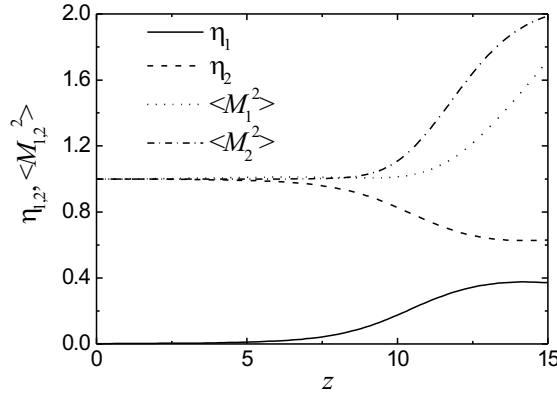


Fig. 6. Dependences of the energy conversion efficiencies and the beam propagation factors on the distance inside the crystal for fundamental and second harmonic pulses.

reconversion to the second harmonic starts, i.e. the conversion efficiency starts to decline. In this specific area, the quality of the fundamental harmonic pulses characterized by the beam propagation factor $\langle M_1^2(z, t) \rangle \approx 1.7$ degrades abruptly. Definition of the propagation factors and their detailed discussion are presented in [4, 27] published earlier in this journal. Therefore, we will not discuss this characteristic of the beams in any more details here. We shall note only that by transmitting the beams through the centered diaphragms possessing the Gaussian transmission $T_G(r) = H_{out}(r, z)/H_{in}(r, z) = \exp[-(r^2/w_G^2)]$ of the energy density $H(r, z)$ of the pulses, the beam quality can be considerably improved, of course, with certain energy losses. However, in this case, it is

especially important that the pulses can be obtained not only with the improved spatial structure, but with significantly shorter duration. Fig. 7 presents the temporal shapes of the pulses propagated through the diaphragms of various radii. It is seen that at the diaphragm radius $w_G/w_{10} = 0.5$, it transmits

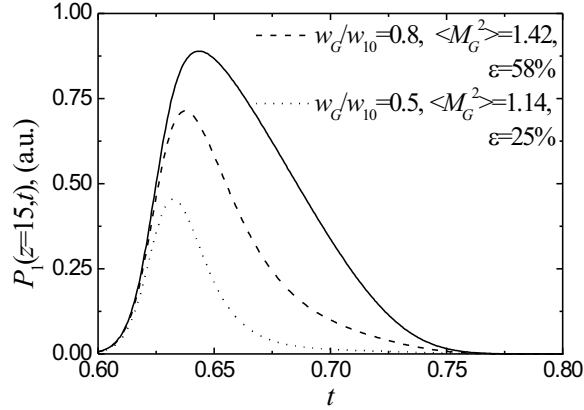


Fig. 7. Envelopes of the fundamental harmonic pulse power $P_1(z = 15, t)$ before (solid curve) and behind the Gaussian diaphragms of different radii.

$\varepsilon = 25\%$ of FH pulse energy. Taking into account that approximately 40% of the second harmonic energy is converted into the fundamental harmonic pulse, $\sim 10\%$ of the second harmonic energy remains in the exit pulse whose duration is approximately 1.5 times shorter than that of the incident pulse. Consequently, a considerable energy amplification (~ 40 times) is achieved with only a slight degradation of the beam quality ($\langle M_1^2(z, t) \rangle \approx 1.14$) and shortening by a factor of ~ 1.5 .

4 Conclusion

As a result of the performed research, an efficient algorithm has been developed for calculations of the optical parametric amplification of the fundamental harmonic at type I phase matching, providing the possibility to optimize the amplification process taking into account the influence of diffraction, group velocity mismatch and dispersion of the FH and SH pulses, with the intention to obtain the exit pulses with the desired parameters. The specific calculations

have demonstrated that in case when the fundamental harmonic pulse being amplified is significantly shorter than the second harmonic pulse, the pulse being amplified shortens noticeably at the beam axis, therefore, by separating the central part of the beam by a soft diaphragm, a significant shortening of the fundamental harmonic pulses is possible.

References

1. Valiulis G., Stabinis A. "Compression of ultrashort light pulses in nonlinear crystals by frequency mixing under conditions strong energy exchange", *Lithuanian J. Phys.*, **31**(1), p. 34–37, 1991
2. Valiulis G., Stabinis A. "Sum-frequency pulse compression by means of phase-conjugated waves mixing in nonlinear crystals", *Lithuanian J. Phys.*, **31**(2), p. 117–120, 1991
3. Stabinis A., Valiulis G., Ibragimov E.A. "Effective sum frequency pulse compression in nonlinear crystals," *Opt. Commun.*, **86**(3–4), p. 301–306, 1991
4. Kurtinaitis A., Dement'ev A., Ivanauskas F. "Modeling of pulse propagation factor changes in type II second-harmonic generation", *Nonlinear Analysis: Modelling and Control*, **6**(2) p. 51–69, 2001
5. Dubietis A., Jonušauskas G., Piskarskas A. "Powerful femtosecond pulse generation by chirped and stretched pulse parametric amplification in BBO crystal", *Opt. Commun.*, **88**(4–6), p. 437–440, 1992
6. Ross I.N., Matousek P., Towrie M., Langley A.J., Collier J.L. "The prospects for ultrashort pulse duration and ultrahigh intensity using optical parametric chirped pulse amplifiers", *Opt. Commun.*, **144**(1–3), p. 125–133, 1997
7. Matousek P., Rus B., Ross I.N. "Design of a multi-petawatt optical parametric chirped pulse amplifier for the iodine laser ASTERIX IV", *IEEE J. Quantum Electron.*, **36**(2), p. 158–163, 2000
8. Ross I.N., Collier J.L., Matousek P., Danson C.N., Neely D., Allott R.M., Pepler D.A., Hernandez-Gomez C., Osvey K. "Generation of terawatt pulses by use of optical parametric chirped pulse amplification", *Appl. Opt.*, **39**(15), p. 2422–2427, 2000
9. Jovanovic I., Comaskey B.J., Ebberts Ch.A., Bonner R.A., Pennington D.M., Morse E.C. "Optical parametric chirped-pulse amplifier as an alternative to Ti:sapphire regenerative amplifiers", *Appl. Opt.*, **41**(15), p. 2923–2929, 2002

10. Yang X., Xu Zh., Leng Y., Lu H., Lin L., Zhang Zh., Li R., Zhang W., Yin D., Tan B. "Multiterawatt laser system based on optical parametric chirped pulse amplification", *Opt. Lett.*, **27**(13), p. 1135–1137, 2002
11. Ross I.N., Matousek P., New G.H.C., Osvey K. "Analysis and optimization of optical parametric chirped pulse amplification", *J. Opt. Soc. Am. B*, **19**(12), p. 2945–2956, 2002
12. Cerullo G., Silvestri D. "Ultrafast optical parametric amplifiers", *Rev. Sci. Instrum.*, **74**(1), p. 1–18, 2003
13. Zhu P., Qian L., Xue Sh., Lin Z. "Numerical studies of optical parametric chirped pulse amplification", *Optics & Laser Technology*, **35**, p. 13–19, 2003
14. Harimoto T., Yamakawa K. "Numerical analysis of optical parametric chirped pulse amplification with time delay", *Opt. Express*, **11**(8), p. 939–943, 2003
15. Harimoto T. "Evaluation of stable optical parametric amplification involving temporal distribution", *Jpn. J. Appl. Phys.*, **42**(6A), p. 3415–3418, 2003
16. Waxer L.J., Bagnoud V., Begishev I.A., Guardalben M.J., Puth J., Zuegel J.D. "High-conversion-efficiency optical parametric chirped-pulse amplification system using spatiotemporally shaped pump pulses", *Opt. Lett.*, **28**(14), p. 1245–1247, 2003
17. Guardalben M.J., Keegan J., Waxer L.J., Bagnoud V., Begishev I.A., Puth J., Zuegel J.D. "Design of a highly stable, high – conversion – efficiency, optical parametric chirped – pulse amplification system with good beam quality", *Optics Express*, **11**(20), p. 2511–2524, 2003
18. Arisholm G., Rustad G., Stenersen K. "Importance of pump – beam group velocity for backconversion in optical parametric oscillators", *J. Opt. Soc.Am.B*, **18**(12), p. 1882–1890, 2001
19. Stegeman G.I., Hagan D.J., Torner L. " $\chi^{(2)}$ cascading phenomena and their applications to all-optical signal processing, mode-locking, pulse compression and solitons", *Optical and Quantum Electronics*, **28**(12), p. 1691–1740, 1996
20. López-Martens R., Fournier S., Le Blanc C., Baubeau E., Salin F. "Parametric amplification and self-compression of ultrashort tunable pulses", *IEEE J. Selected Topics in Quantum Electron.*, **4**(2), p. 230–236, 1998
21. Fournier S., López-Martens R., Le Blanc C., Baubeau E., Salin F. "Solitonlike pulse shortening in a femtosecond parametric amplifier", *Opt. Lett.*, **23**(8), p. 627–629, 1998

22. Liu X., Qian L., Wise F. "Generation of optical spatiotemporal solitons", *Phys. Rev. Lett.*, **82**(23), p. 4631–4634, 1999
23. Liu X., Qian L., Wise F. "High-energy pulse compression by use of negative phase shifts produced by the cascade nonlinearity", *Opt. Lett.*, **24**(23), p. 1777–1779, 1999
24. Wise F., Qian L., Liu X. "Applications of cascaded quadratic nonlinearities to femtosecond pulse generation", *J. Nonlin. Opt. Phys. & Mat.*, **11**(3), p. 317–337, 2002
25. Ashihara S., Nishina J., Shimura T., Kuroda K. "Soliton compression of femtosecond pulses in quadratic media", *J. Opt. Soc. Am. B*, **19**(10), p. 2505–2510, 2002
26. Buryak A.V., Trapani P.D., Skryabin D.V., Trillo S. "Optical solitons due to quadratic nonlinearities: from basic physics to futuristic applications", *Physics Reports*, **370**, p. 63–235, 2002
27. Dementjev A., Girdauskas V., Vrublevskaia O. "Numerical treatment of short laser pulse compression in transient stimulated Brillouin scattering", *Nonlinear Analysis: Modelling and Control*, **7**(1), p. 3–29, 2002
28. Dmitriev V.G., Gurzadyan G.G., Nikogosyan D.N. *Handbook of nonlinear optical crystals*, Springer, New York, 1997
29. Dement'ev A., Girdauskas V., Vrublevskaia O., Kazragyte R. "Numerical investigation of influence of the nonlinear refraction index upon the second harmonic generation", *Lithuanian J. Phys.*, **42**(4), p. 263–274, 2002